ISBN: 978-3-95450-192-2 doi:10.18429/JACoW-IBIC2017-WEPCC09

HORIZONTAL OPENING OF THE SYNCHROTRON RADIATION AND EFFECT OF INCOHERENT DEPTH OF FIELD FOR HORIZONTAL BEAM SIZE MEASUREMENT

T. Mitsuhashi†, KEK, Ibaraki, Japan
J. Corbett, SLAC, Menlo Park, CA, USA
M. J. Boland, SLSA, Clayton, Australia

Abstract

The incoherent depth-of-field due to the instantaneous opening angle of dipole SR emission can influence horizontal beam size measurements. In particular, for double-slit spatial interferometry, the opening angle introduces an intensity imbalance across the two slits that reduces interference contrast and therefore increases the apparent beam size. To investigate this effect, the instantaneous horizontal opening of the SR light must be known. Schwinger's theory gives the vertical opening angle and the qualitative theory of K.J. Kim gives an estimation for horizontal opening angle. An extension of Schwinger's theory to the horizontal plane by one of the authors leads to the same Bessel function distribution as the vertical plane using integration by parts. Neglecting the cubic phase term in the exponent, the expression agrees with Kim's diffraction theory. Using this result to correct for incoherent depth-of-field effects in double-slit measurements at the Australian Synchrotron, ATF and SPEAR3, the measured horizontal beam size is in good agreement with design values.

INTRODUCTION

For the measurement of horizontal beam size, the incoherent depth of field due to horizontal instantaneous opening of the Synchrotron Radiation will modify the spatial coherence in the horizontal direction. In particular, for double-slit spatial interferometry, the opening angle introduces an intensity imbalance across the two slits that reduces interference contrast and therefore increases the apparent beam size. To investigate this effect, the information of instantaneous horizontal opening of the SR light must be known. It is well known that the theory for the Synchrotron radiation which emitted from Circular trajectory is investigated by J. Schwinger, and he gives the vertical opening angle for the spectral density [1]. The qualitative theory of K.J. Kim gives an estimation for both of vertical and horizontal opening angle by using diffraction concept [2]. In this paper, a simple introduction for K.J. Kim's paradigm and Schwinger's theory, then we discuss an extension of Schwinger's theory to the horizontal plane using integration by parts. Using this result to correct for incoherent depth-of-field effects in double-slit measurements at the SPEAR3, Australian Synchrotron and ATF, the measured horizontal beam size is in good agreement with design values.

EFFECT OF INCOHERENT DEPTH OF FILED FOR HORIZONTAL INTERFEROMETRY

In the horizontal plane, the interferogram includes the additional effect of incoherent depth of field (IDOF) by the instantaneous opening of the SR in the horizontal plane [3][4]. The IDOF has two effects, the first is the apparent horizontal beam size becomes bigger and the second is the visibility of the horizontal interferogram reduces by intensity imbalance at two opening of double slit. Using the instantaneous intensity distribution of SR in horizontal plane by $I(\theta)$ as a function of horizontal observation angle θ, the apparent beam shape $\sigma_\alpha(x)$ including the intensity imbalance factor is given by,

$$\sigma_a(x)=\int \frac{2\sqrt{I\left(\theta+\frac{D}{2R}\right)I\left(\theta-\frac{D}{2R}\right)}}{I\left(\theta+\frac{D}{2R}\right)+I\left(\theta-\frac{D}{2R}\right)}\cdot I(\theta)\cdot\frac{\exp\left[\frac{-\left[x-\rho\{1-\cos(\theta)\}\right]^2}{2\sigma^2}\right]}{\sigma\cdot\sqrt{2\pi}}d\vartheta \tag{1}$$

where the original beam profile is assumed to be ~~a~~ Gaussian. The visibility of the interferogram γ_h (D) is given by Fourier cosine transform of the apparent beam shape as follows,

$$\gamma_h(D)=\int \sigma_a(x)\cdot\cos\left(\frac{2\pi\cdot D\cdot x}{R\cdot\lambda}\right)dx \tag{2}$$

For the discussion of horizontal spatial coherence, we need knowledge of instantaneous intensity distribution of SR in horizontal plane.

HORIZONTAL INSTANTANEOUS SR OPENING BY K.J.KIM

A horizontal instantaneous opening of the SR is qualitatively discussed by K. J. Kim [2]. He considers an apparent shape of circular trajectory by using time scale change factor (Doppler factor) as indicated in Fig. 1. According to his paradigm, the kink shaped apparent trajectory due to strong temporal squeezing in observer

†email address: toshiyuki.mitsuhashi@kek.jp

ISBN: 978-3-95450-192-2 doi:10.18429/JACoW-IBIC2017-WEPCC09

time radiate the Synchrotron Radiation. The radiation is propagating with the diffraction by kink size.

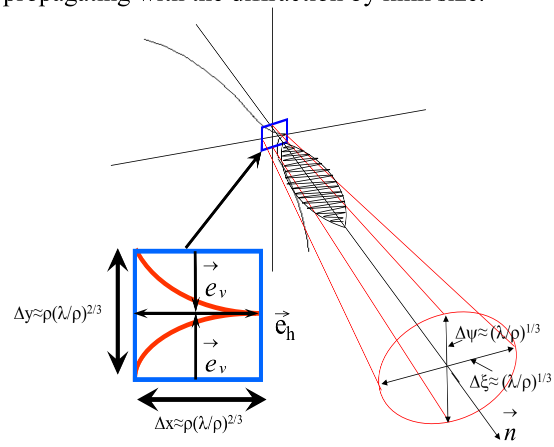

Figure 1: Apparent shape of circular trajectory by using time scale change factor (Doppler factor).

The horizontal and vertical sizes of the kink are given by

$$\Delta \boldsymbol{x} \approx \rho\left(\frac{\lambda}{\rho}\right)^{2/3} \quad , \quad \Delta \boldsymbol{y} \approx \rho\left(\frac{\lambda}{\rho}\right)^{2/3} \qquad (3)$$

Then, the horizontal opening $\Delta\xi$ and vertical opening $\Delta\psi$ of radiation is given by diffraction of this source size,

$$\Delta\xi \approx (\lambda/\rho)^{1/3} \quad , \quad \Delta\psi \approx (\lambda/\rho)^{1/3} \qquad (4)$$

These results indicate instantaneous horizontal opening of the SR is same as vertical opening.

In next chapter, let us discuss quantitative theory by extending the Schwinger's theory for SR.

EXTENSION OF SCHWINGER'S THEORY TO HORIZONTAL INSTANTANEOUS SR OPENING

The SR from circular trajectory is written by Schwinger in 1945 [1]. He only gave his theory for horizontal observation angle ξ=0. Before discuss the general case, $\xi\neq0$, let us simply refer the Schwinger's theory for horizontal observation angle ξ=0.

Let us start the vector potentials for parallel and perpendicular components of the radiation as follows,

$$\mathbf{A}_{\parallel}(\omega) \cong \frac{c}{\rho}\int_{-\infty}^{\infty} \boldsymbol{t'} \boldsymbol{exp}\left\{\boldsymbol{i}\frac{\omega}{\boldsymbol{2}}\left[\left(\frac{\boldsymbol{1}}{\gamma^2}+\psi^2+\xi^2\right)\boldsymbol{t'}+\frac{\boldsymbol{c^2}}{\boldsymbol{3}\rho^2}\boldsymbol{t'^3}+\frac{c}{\rho}\xi\,\boldsymbol{t'^2}\right]\right\}\boldsymbol{dt'} \qquad (5)$$

$$\mathbf{A}_{\perp}(\omega) = \psi\int_{-\infty}^{\infty} \boldsymbol{exp}\left\{\boldsymbol{i}\frac{\omega}{\boldsymbol{2}}\left[\left(\frac{\boldsymbol{1}}{\gamma^2}+\psi^2+\xi^2\right)\boldsymbol{t'}+\frac{\boldsymbol{c^2}}{\boldsymbol{3}\rho^2}\boldsymbol{t'^3}+\frac{c}{\rho}\xi\,\boldsymbol{t'^2}\right]\right\}\boldsymbol{dt'} \qquad (6)$$

Putting the horizontal observation angle ξ=0. The vector potentials becomes

$$\mathbf{A}_{\parallel}(\omega) \cong \frac{c}{\rho}\int_{-\infty}^{\infty} t'\exp\left\{i\frac{\omega}{2}\left[\left(\frac{1}{\gamma^2}+\psi^2\right)t'+\frac{c^2}{3\rho^2}t'^3\right]\right\}dt' \qquad (7)$$

$$\mathbf{A}_{\perp}(\omega) = \psi\int_{-\infty}^{\infty} \exp\left\{i\frac{\omega}{2}\left[\left(\frac{1}{\gamma^2}+\psi^2\right)t'+\frac{c^2}{3\rho^2}t'^3\right]\right\}dt' \qquad (8)$$

After some change of variables, and using Airy integrals, and alternatively as modified Bessel functions, consequently the intensity radiated per unit frequency interval per unit solid angle is given by

$$\frac{d^2 I}{d\omega d\Omega} = \frac{e^2}{3\pi^2 c}\left(\frac{\omega\rho}{c}\right)^2\left(\frac{1}{\gamma^2}+\psi^2\right)^2\left[K_{2/3}^2(\zeta)+\frac{\psi^2}{\frac{1}{\gamma^2}+\psi^2}K_{1/3}^2(\zeta)\right] \qquad (9)$$

Where

$$\zeta = \frac{\omega\rho}{3c}\left(\frac{1}{\gamma^2}+\psi^2\right)^{\frac{3}{2}} \qquad (10)$$

The intensity distribution as a function of vertical observation angle is indicated in Fig. 2 for SR at wavelength of 500nm. This calculation is using the condition of bending magnet at Australian Synchrotron.

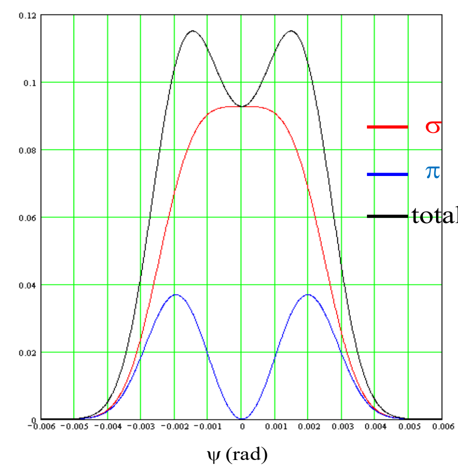

Figure 2: The intensity distribution as a function of vertical observation angle.

Let us move on to general case for horizontal observation angle $\xi\neq0$. Return to vector potential of parallel component, Eq. (5), rewritten exponent into the product of linear + cubic term of t' and quadratic term of t' the vector potential becomes,

$$\mathbf{A}_{\parallel}(\omega) \cong \frac{c}{\rho}\int_{-\infty}^{\infty} \boldsymbol{t'} \boldsymbol{exp}\left\{\boldsymbol{i}\frac{\omega}{\boldsymbol{2}}\left[\left(\frac{\boldsymbol{1}}{\gamma^2}+\psi^2+\xi^2\right)\boldsymbol{t'}+\frac{\boldsymbol{c^2}}{\boldsymbol{3}\rho^2}\boldsymbol{t'^3}+\frac{c}{\rho}\xi\,\boldsymbol{t'^2}\right]\right\}\boldsymbol{dt'}$$

$$= \frac{c}{\rho}\int_{-\infty}^{\infty} \boldsymbol{t'} \boldsymbol{exp}\left\{\boldsymbol{i}\frac{\omega}{\boldsymbol{2}}\left[\left(\frac{\boldsymbol{1}}{\gamma^2}+\psi^2+\xi^2\right)\boldsymbol{t'}+\frac{\boldsymbol{c^2}}{\boldsymbol{3}\rho^2}\boldsymbol{t'^3}\right]\right\}$$

$$\cdot\,\boldsymbol{exp}\left\{\boldsymbol{i}\frac{\omega}{\boldsymbol{2}}\frac{c}{\rho}\xi\,\boldsymbol{t'^2}\right\}\boldsymbol{dt'} \qquad (11)$$

Then, integrating the vector potential by parts gives,

ISBN: 978-3-95450-192-2 doi:10.18429/JACoW-IBIC2017-WEPCC09

$$\mathbf{A}_{\parallel}(\omega) \cong \frac{c}{\rho}\left[\int_{-\infty}^{\infty} t' exp\left\{i\frac{\omega}{2}\left[\left(\frac{1}{\gamma^2}+\psi^2+\xi^2\right)t'+\frac{c^2}{3\rho^2}t'^3\right]\right\}dt' \cdot exp\left\{i\frac{\omega}{2}\frac{c}{\rho}\xi t'^2\right\} + \int_{-\infty}^{\infty} f(t')\cdot i\frac{\omega}{2}\xi\frac{c}{\rho}\frac{1}{2}t'\cdot exp\left\{i\frac{\omega}{2}\xi\frac{c}{\rho}t'^2\right\}dt'\right] \tag{12}$$

Where $f(t')$ is,

$$f(t') = \int_{-\infty}^{\infty} t' \exp\left\{i\frac{\omega}{2}\left[\left(\frac{1}{\gamma^2}+\psi^2+\xi^2\right)t'+\frac{c^2}{3\rho^2}t'^3\right]\right\}dt' \tag{13}$$

The same way to derive Eq. (9) from Eq. (8), $f(t')$ can replaced by modified Bessel function $K_{2/3}$. The second term in right hand of Eq. (12) becomes,

$$i\frac{\omega}{2}\xi\frac{c}{\rho}\frac{1}{2}\mathrm{a}\cdot K_{2/3}\int_{-\infty}^{\infty} t' exp\left\{i\frac{\omega}{2}\xi\frac{c}{\rho}t'^2\right\}dt' \tag{14}$$

This integral is Fresnel transform of odd function t', and it becomes zero. Then, the vector potential becomes,

$$\mathbf{A}_{\parallel}(\omega) \cong \frac{c}{\rho}\int_{-\infty}^{\infty} t' \exp\left\{i\frac{\omega}{2}\left[\left(\frac{1}{\gamma^2}+\psi^2+\xi^2\right)t'+\frac{c^2}{3\rho^2}t'^3\right]\right\}dt' \cdot \exp\left\{i\frac{\omega}{2}\frac{c}{\rho}\xi t'^2\right\} \tag{15}$$

The quadratic phase term in right hand of this equation,

$$\exp\left\{i\frac{\omega}{2}\frac{c}{\rho}\xi t'^2\right\} \tag{16}$$

Since phase term having unit amplitude becomes 1 after calculating intensity (absolute value), so we can neglect this constant phase term from the vector potential. We can write the vector potential for parallel component as follows,

$$\mathbf{A}_{\parallel}(\omega) \cong \frac{c}{\rho}\int_{-\infty}^{\infty} t' \exp\left\{i\frac{\omega}{2}\left[\left(\frac{1}{\gamma^2}+\psi^2+\xi^2\right)t'+\frac{c^2}{3\rho^2}t'^3\right]\right\}dt' \tag{17}$$

In the same way, the vector potential for perpendicular component is given by,

$$\mathbf{A}_{\perp}(\omega) \cong \psi\int_{-\infty}^{\infty} \exp\left\{i\frac{\omega}{2}\left[\left(\frac{1}{\gamma^2}+\psi^2+\xi^2\right)t'+\frac{c^2}{3\rho^2}t'^3\right]\right\}dt' \tag{18}$$

The intensity radiated per unit frequency interval per unit solid angle is given by

$$\frac{d^2I}{d\omega\, d\Omega} = \frac{e^2\omega^2}{4\pi^2 c}\left|\mathbf{A}_{\parallel}(\omega)+\mathbf{A}_{\perp}(\omega)\right|^2 \tag{19}$$

After some change of valiables, and using Airy integrals, and alternatively as modified Bessel functions, consequently the intensity radiated per unit frequency interval per unit solid angle is given by

$$\frac{d^2I}{d\omega d\Omega} = \frac{e^2}{3\pi^2 c}\left(\frac{\omega\rho}{c}\right)^2\left(\frac{1}{\gamma^2}+\psi^2+\xi^2\right)^2\left[K_{2/3}^2(\zeta)+\frac{\psi^2}{\frac{1}{\gamma^2}+\psi^2+\xi^2}K_{1/3}^2(\zeta)\right] \tag{20}$$

Where,

$$\zeta = \frac{\omega\rho}{3c}\left(\frac{1}{\gamma^2}+\psi^2+\xi^2\right)^{\frac{3}{2}} \tag{21}$$

The result given by Eq.(20) indicates both of vertical intensity distribution and horizontal instantaneous intensity distribution have same angular dependence. This result is same as in the result from qualitative discussion in K.J. Kim.

SOME CALCULATION FOR HORIZONTAL INTENSITY DISTRIBUTION

Some calculation for intensity distribution using Eq.(20) was performed at several vertical observation angle.
Results are shown in Fig. 3. In this calculation, the condition of bending magnet of SPEAR 3 in SLAC was used.

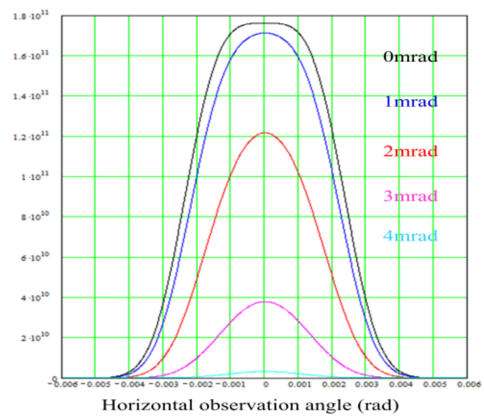

Figure 3: Horizontal intensity distribution of SR at several vertical observation angle.

To see the intensity destitution by modified Bessel function, the normalized intensity plots are shown in Fig. 4.

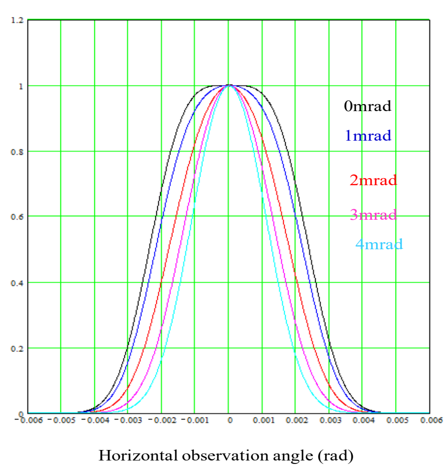

Figure 4: Normalized intensity distribution at several vertical observation angle.

ISBN: 978-3-95450-192-2 doi:10.18429/JACoW-IBIC2017-WEPCC09

To see Fig. 4, Intensity distributions for each vertical observation angle has different distribution, because of the distribution is given by modified Bessel function. To watch two dimensional distribution of radiation written by eq. (20), two dimensional plot is indicated in Fig. 5.

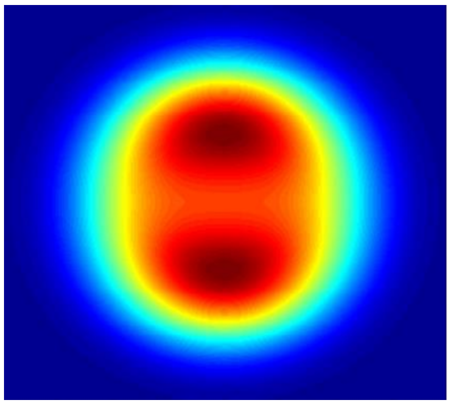

Figure 5: Two dimensional plot of Eq. (20).

HORIZONTAL BEAM SIZE MEASUREMENT USING HORIZAONTAL INTENSITY DISTRIBUTION

Horizontal beam size measurements are performed including the IDOF effect and horizontal intensity distribution at SPEAR3, ALS, and ATF [6].

Result the visibility at SPEAR3 as a function of the slit separation is shown in Fig. 6 [5][6]. Two analysis methods, one is including the IDOF and other is not including IDOF are shown in this figure. The result of horizontal beam size is 132.7μm. Due to a large horizontal beam size, the effect of IDOF is rather small.

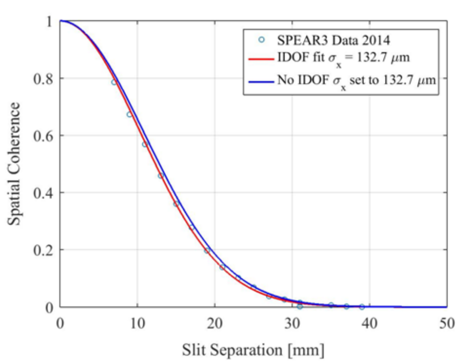

Figure 6: Horizontal visibility measured at SPEAR 3 as a function of slit separation.

The second is a measurement at the Australian Synchrotron ALS [6]. The measured horizontal visibility is shown in Fig. 7 and the horizontal beam size taking IDOF into account is 88μm. Due to a smaller horizontal beam size at the source point the effect of IDOF is larger than at SPEAR3.

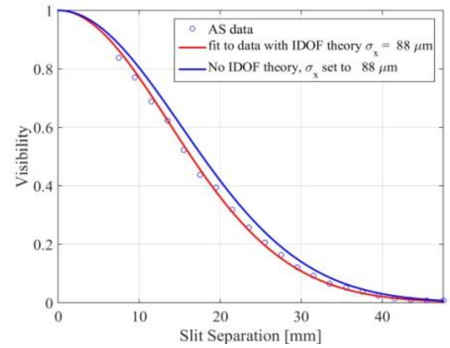

Figure 7: Horizontal visibility measured at ALS as a function of slit separation.

The third is a measurement at the ATF [7]. The measured horizontal visibility is shown in Fig. 8 and the horizontal beam size taking IDOF into account is 38.5μm. Due to smaller horizontal beam size, the effect of IDOF is the largest in these tree measurements.

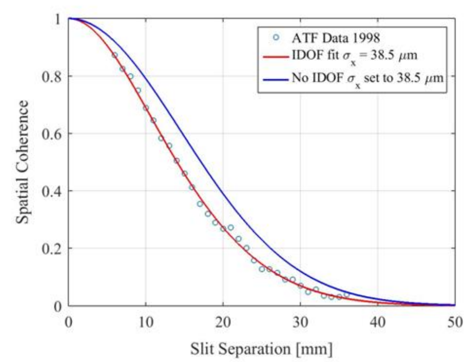

Figure 8: Horizontal visibility measured at ATF as a function of slit separation.

In each case, the results for horizontal beam sizes are in good agreement with designed values when the IDOF effect with horizontal intensity distribution is taken into account.

CONCLUSIONS

The horizontal intensity distribution of SR from circular trajectory is investigated by extending Schwinger's theory for SR. As a result, we derived the same Bessel function distribution as in the vertical plane for the horizontal intensity distribution. The IDOF effect for horizontal beam size measurement via interferometry including the horizontal intensity distribution is investigated by through the measured visibility at SPEAR3, ALS and ATF. For the three measurements, the results for horizontal beam size measurements are in good agreement with designed values when the IDOF effect with horizontal intensity distribution is included.

ACKNOWLEDGEMENT

Authors acknowledge to Prof. Oide of CERN for helpful discussion and his encourage for this work. Thanks also due to Dr. Georges Trad of CERN for his calculation of two dimensional distribution of SR intensity.

ISBN: 978-3-95450-192-2 doi:10.18429/JACoW-IBIC2017-WEPCC09

REFERENCES

[1] J. Schwinger, "On Radiation by Electron in a Betatron", published in A quantum Legacy : Seminal paper of J. Schwinger, World Scientific,p.307 (2000). Also see J. Schwinger, Phys.Rev.75p.1912 (1949)

[2] K.J. Kim, "Characteristics of Synchrotron Radiation", in AIP conference proceedings 184, p565 (1989).

[3] T. Mitsuhashi, "Beam Profile and Size Measurement by SR Interferometer" in Beam measurement, Ed. by S.Kurokawa *et al.*, 399-427,World Scientific(1999).

[4] T.Mitsuhashi, Proceedings of IPAC2015, p3663, (2015).

[5] Jeff Corbett, private communication.

[6] M. Boland, Jeff Corbett and T. Mitsuhashi, Proc. Of IPAC 2015, p1391, (2015).

[7] T. Naito and T. Mitsuhashi, Phys. Rev. ST Accel. Beams 9, 122802 (2006).